Author(s): Ayuela, A. & Raebiger, H. & Puska, M. J. & Nieminen, Risto M.

Title: Spontaneous magnetization of aluminum nanowires deposited on the NaCl(100) surface

Year: 2002

Version: Final published version

**Please cite the original version:**

Ayuela, A. & Raebiger, H. & Puska, M. J. & Nieminen, Risto M. 2002. Spontaneous magnetization of aluminum nanowires deposited on the NaCl(100) surface. Physical Review B. Volume 66, Issue 3. 035417/1-8. ISSN 1550-235X (electronic). DOI: 10.1103/physrevb.66.035417.

# Spontaneous magnetization of aluminum nanowires deposited on the NaCl(100) surface

A. Ayuela, H. Raebiger, M. J. Puska, and R. M. Nieminen
*Laboratory of Physics, Helsinki University of Technology, 02015 Espoo, Finland*
(Received 27 March 2002; published 26 July 2002)

We investigate electronic structures of Al quantum wires, both unsupported and supported on the (100) NaCl surface, using the density-functional theory. We confirm that unsupported nanowires, constrained to be linear, show magnetization when elongated beyond the equilibrium length. Allowing ions to relax, the wires deform to zigzag structures with lower magnetization but no dimerization occurs. When an Al wire is deposited on the NaCl surface, a zigzag geometry emerges again. The magnetization changes moderately from that for the corresponding unsupported wire. We analyze the findings using electron band structures and simple model wires.

DOI: 10.1103/PhysRevB.66.035417 PACS number(s): 73.21.Hb, 75.75.+a, 68.65.La

## I. INTRODUCTION

Electronic properties of nanowires adsorbed on solid surfaces depend strongly on the geometric structure of the wire. The surface enables the realization of a specific geometry but the interaction between the substrate and the adsorbed wire does not necessarily destroy the key properties the wire would have in the same geometry when isolated. This idea has been the basis of many recent experimental and theoretical studies of nanowires on semiconducting[1–5] and metallic[6,7] substrates. The studies of nanowires on surfaces have been motivated from the new technology point of view. Nanowires can be seen as ultimate leads when miniaturizing devices in electronics. Moreover, if they exhibit magnetization they could be used as compact magnetic storage devices. In general, the exciting quantum phenomena taking place as the size and the dimensionality of the system are reduced are the driving force in the research of nanostructures.

The manufacturing of nanowires on solid surfaces can be based on the manipulation of the surface and the adsorbate atoms with the scanning tunneling microscope (STM).[8,9] A more efficient method for fabrication may be the deposition of adsorbate atoms in the steps on metal surfaces[10,11] or the growing of stripelike adsorbate structures either on metal[6,12] or on semiconductor[2,4,5] surfaces. The geometry of these structures can be monitored using a STM,[4,10,13] He scattering,[10] or by a field ion microscope.[12] An efficient way to characterize the electronic structures of wires, e.g., their one dimensionality, is angle-resolved photoemission.[2,5,6]

In this work we report state-of-the-art electronic structure calculations based on the density-functional theory (DFT) for simple metal nanowires on an insulating substrate, i.e., for Al wires on the NaCl(100) surface. The present work is largely inspired by the theoretical investigations of Ga adsorbate wires on Si(100) surface performed by Watanabe *et al.*[14] Using first-principles electronic structure methods they calculated the stable structures of Ga-dangling-bond wires on hydrogen-terminated Si(100). The resulting band structures show that the wires are metallic and that in some of the structures the adsorbate-induced band near the Fermi level is very flat. On this basis Watanabe *et al.*[14] discussed, using a simple tight-binding model, the possibility of ferromagnetism in these simple metal wires. Recently, Okada and Oshiyama[15] returned to these Ga wires on Si(100) performing first-principles DFT calculations. They found one atomic configuration for the Ga wire exhibiting ferromagnetic ordering. We have chosen to work with Al wires because the jellium model calculations[16] have predicted, and the subsequent first-principles calculations[17] have confirmed, that isolated linear Al-atom chains can be magnetic for certain interatomic distances. NaCl has been selected as the substrate due to its insulating character, which is expected to be reflected as minor substrate effects in the electron structure of the Al wire, and due to the fact that the atomic distances on the NaCl(100) surface match with the interatomic distance of a magnetic isolated Al chain. This surface is also expected to be stable, as a surface reconstruction occurs only in one of many different cleavages.[18] An Al wire on the unreconstructed NaCl surface is a much simpler system than Ga wires on the hydrogenated reconstructed Si(100). Therefore the present calculations are expected to show clearly the essential physical phenomena for simple metal wires on insulating surfaces. Because the properties of a nanowire on a surface are largely derived from those of unsupported wires, we begin this work by calculations for isolated wires in different geometries and study their properties as functions of structural parameters.

The organization of the present paper is as follows. In Sec. II we discuss the computational details. We use the Vienna *ab initio* simulation package[19] (VASP), which is a pseudopotential-plane-wave (PPPW) code. Moreover, we have made benchmark calculations using the full-potential linearized augmented plane-wave (FLAPW) method with the WIEN97 package.[20] FLAPW is considered more accurate but it is also much more CPU-time consuming than the PPPW method. In Sec. III we present our results, first for the unsupported linear (Sec. III A) and dimerized or zigzag wires (Sec. III B) and thereafter for wires on the NaCl(100) surface (Sec. III C). Section IV summarizes our results and includes an outlook.

## II. COMPUTATIONAL DETAILS

We employ in our DFT electronic structure calculations the generalized gradient approximation (GGA) for the exchange-correlation effects.[21] When describing interactions

 

between adsorbate atoms and a substrate it has been found important to go beyond the local-density approximation (LDA). We do both spin-polarized and spin-compensated computations in order to find the solution of the lowest energy.

In the PPPW calculations (VASP) we have used ultrasoft Vanderbilt pseudopotentials.[22] In the case of unsupported Al wires the cutoff energy of the plane-wave expansion has been 180 eV. This is sufficient to describe bulk Al. In the case of the NaCl surface we need a cutoff energy of 250 eV.

We use the supercell approximation in our calculations. This means that instead of isolated atomic chains, a set of parallel chains are used. In the case of linear chains the interchain distance of 15 Å is sufficient to eliminate the interaction between the wire and its periodic replicas. The zigzag chains are treated in a supercell with the lattice constant of 20 Å perpendicular to the chain axis. In the NaCl(100) surface calculations we have used the slab geometry with one or two layers of Na and Cl atoms. The use of one layer is found sufficient to describe the energetics of straight Al wires on the surface. The NaCl slabs are separated by a vacuum region of 20 Å. On the surface, the Al wires are separated by three lattice constants of NaCl. These separations were found to depress sufficiently the interactions between the slabs or the Al wires. Dipole corrections for the electrostatics of the supercell geometry are also included.[23]

The desired periodicity along the wire and the artificial periodicity due to the supercell approximation require a Brillouin-zone integration. In order to describe correctly the magnetic properties the **k**-point sampling in the wire directions has to be dense enough. We have used 26 **k** points for this purpose. In the case of unsupported wires there are **k** points only on the $k_z$ axis in the wire direction. When calculating Al wires on the NaCl(100) surface the **k** points form a $3\times26$ mesh on the $(k_x,k_z)$ plane parallel to the surface and there are actually 26 **k** points in the irreducible wedge of the Brillouin zone. The Fermi smearing of 0.06 eV is used in the integrations.

In order to test the accuracy of the PPPW calculations, especially with respect to the predicted magnetic properties, we have performed calculations also with the FLAPW method (WIEN97 code) for the unsupported linear Al-atom chain. The FLAPW method can be considered as one of the most accurate band-structure methods. In the calculations, the muffin-tin sphere radii for Al are 2.10 a.u. Inside the muffin-tin spheres the maximum angular momentum $l$ in the radial expansion is $l_{max}=10$, and the largest $l$ value for the nonspherical part of the Hamiltonian matrix is $l_{max,ns}=4$. The cutoff parameters are $RK_{max}=9$ for the plane waves, the number of plane waves ranges up to around 4000. The Brillouin-zone integrations are done using ten special points,[24] and a Fermi broadening of 0.001 Ry is used.

Choosing the above plane-wave cutoff parameters and the maximum angular momenta for basis sets results in total energies, bond distances, and band structures which have numerically converged within 1 meV, 0.01 Å, and 1 meV, respectively, both in the PPPW and in the FLAPW calculations. The **k**-point samplings chosen resulted in magnetic moments converged better than $0.01\mu_B$. The supercell sizes have been checked with respect to the changes in atomic positions and total energies, with convergence better than 0.05 Å and 0.01 eV, respectively. Especially, this is true for the use of two layers of Na and Cl atoms, which is in accord with the calculations of Ref. 28 for Ag atoms adsorbed on MgO.

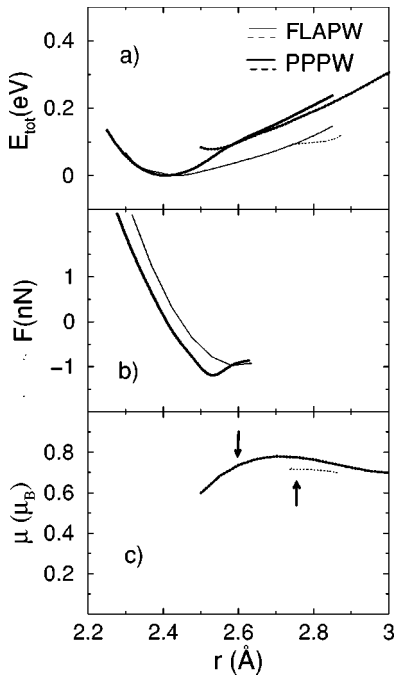


FIG. 1. Total energy (a), elongation force (b), and magnetic moment (c) per atom for an infinite linear chain of Al atoms as a function of the interatomic distance. The FLAPW and PPPW results are denoted by thin and thick lines, respectively. In panel (a), the minimum energy defines the energy zero and the results of spin-compensated and spin-polarized calculations are given by solid and dashed lines, respectively. The arrows in panel (c) indicate points where the spin-polarized states become in elongation more stable than the spin-compensated ones.

## III. RESULTS

### A. Unsupported linear Al wire

First we want to test the accuracy of the pseudopotential approach by comparing the PPPW and FLAPW results in the simple case of an unsupported linear chain of Al atoms. The total energies $E_{tot}$ per atom are shown in the uppermost panel of Fig. 1 as a function of the bond length. The energy minima correspond to spin-compensated solutions. According to the FLAPW method the energy minimum occurs at $d_{nn}=2.43$ Å, which is in a fair agreement with the PPPW result of 2.41 Å. The equilibrium force constants $k=d^2E_{tot}/da^2$ are 104 N/m (FLAPW) and 151 N/m (PPPW). Our GGA-PPPW values are quite close to the LDA results obtained by Mehrez and Ciraci[25] using a PPPW method. According to Fig. 1 the difference between the FLAPW and PPPW results increases towards to the larger interatomic distances. This reflects some difficulties in the transferability of the pseudopotential for larger distances and low dimension-

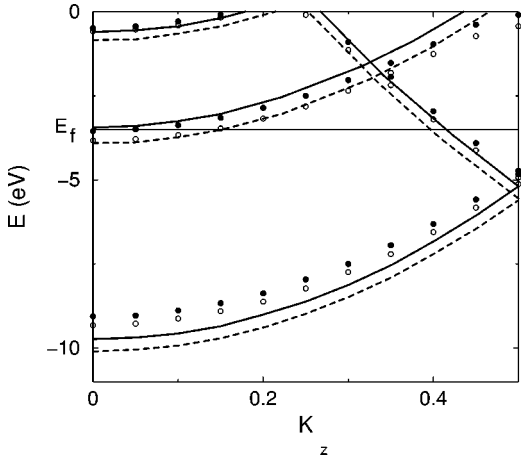


FIG. 2. Band structure of an unsupported linear chain of Al atoms. The interatomic distance is the Al bulk bond distance of $d_{nn}=2.86$ Å. The results of the FLAPW calculation are denoted by open and filled circles for the majority- and minority-spin bands, respectively. The properly folded subband structure of an infinitely long stabilized-jellium wire with $r_s=2.07$ a.u. and radius of 1.35 Å is shown as dashed and solid lines corresponding to the majority and minority spins, respectively. The Fermi level is given by the horizontal thin line.

ality, because the increase of the energy cutoff does not change the PPPW results substantially.

The stabilized-jellium model calculations have predicted that nanowires of simple metals may be magnetic.[16] In Fig. 1 the results obtained using the spin-compensated formalism are connected with solid lines whereas solutions with magnetic moments are connected with dashed lines. At distances larger than 2.7 Å (FLAPW) or 2.6 Å (PPPW) the total energy of a magnetic solution is indeed lower than that of the spin-compensated one. The magnetic solution is due to the spin polarization of the second subband accommodating atomic $3p$ electrons (see Fig. 2). In the bottom panel of Fig. 1 the resulting magnetic moment per atom is given as a function of the elongation. The magnetic moments calculated by both methods saturate to a value around $0.7\mu_B$ per Al atom. It is interesting to compare this value with the stabilized-jellium model prediction, which gives, corresponding to the interatomic distance of 2.86 Å (bond length in bulk Al), a moment of $0.65\mu_B$ per Al atom.[26]

The elongation force is defined as the force opposing the lengthening of the wire due to an external applied force. When negative, the elongation force would like to shorten the wire, whereas a positive elongation force without a counterbalancing force would lead to a spontaneous elongation. In the case of a linear atomic chain, the elongation force is calculated as

$$F=-\frac{dE_{tot}}{dr}, \tag{1}$$

where $r$ is the interatomic distance. Naturally, the force vanishes at the minimum energy and is negative for larger distances. For very large distances the force should approach zero. The crucial point is that when the wire is stretched, the force reaches a minimum, which determines the maximum force sustained before breaking. In both calculations, the breaking force is about 1.5 nN. This is of the same magnitude as the typical force before breaking seen in the atomic force microscope experiments[27] on gold nanowires. According to Fig. 1 the breaking of the linear Al chain occurs as a function of the elongation before the magnetization sets in. If the chain would be stable, the onset of the magnetization should result in a discontinuous decrease of the magnitude of the elongation force.[16]

It is instructive to compare the one-dimensional band structure of the linear Al chain with the properly folded subband structure of an infinitely long stabilized-jellium cylinder. This is done in Fig. 2. The Al chain is calculated using FLAPW for the interatomic distance of 2.86 Å. The splitting of the bands due to the magnetic ground state occurs at this distance. The PPPW method gives quantitatively similar results. In the stabilized-jellium calculation[26] the density $n$ of the positive jellium charge corresponds to the electron-density parameter $r_s=(3/4\pi n)^{1/3}=2.07$ a.u. The radius, 1.35 Å, of the positive background charge is chosen to give the linear charge density of $3e/2.86$ Å. The electronic structure has been solved self-consistently within the LDA. The above value of the jellium radius falls in a narrow window, in which the the second, doubly degenerate subband, corresponding to the quantum numbers $m=1$ and $n=1$, is totally spin polarized resulting in the magnetic solution. In the atomic chain calculations the corresponding, nearly totally polarized band arises from the atomic $p_{xy}$ orbitals (the $z$ axis is parallel to the chain). In a quasi-one-dimensional system the density of states (DOS) diverges at the bottom of a subband. When the Fermi level is just above the bottom of a subband, the Fermi-level DOS will be large and the system will fulfill the Stoner criterion for magnetism.[16] The quantum numbers of the lowest jellium subband are $m=0$ and $n=1$. The corresponding atomic chain states have the character of the atomic $3s$ orbital on the lowest branch, and after the band is folded at $k_z=\pi/a$ the character is that of the atomic $3p_z$ orbitals. The contribution of the lowest subband to the magnetic moment of the wire is small in comparison with the second (nearly) totally polarized subband. The agreement between the jellium and atomic chain models is surprisingly good. This gives credence to the stabilized-jellium model for Al even in the present very confined geometry.

In conclusion, in the case of the unsupported linear chain of Al atoms the PPPW calculations are able to reproduce the essential cohesive properties obtained in the all-electron FLAPW calculation. Also the magnetic properties, which are of a especial interest in the preset work, are similar in both calculations. The onset distances of the spontaneous magnetization differ by ~5% and the magnetic moments by $\sim 0.05\mu_B$ between the two calculations. These differences are of the same order of magnitude as those expected to result from approximating the exchange-correlation effects. Therefore in the following calculations for the unsupported dimerized and zigzag Al wires as well as for the Al wires on the NaCl (100) surface we rely on the less computer intensive PPPW method.

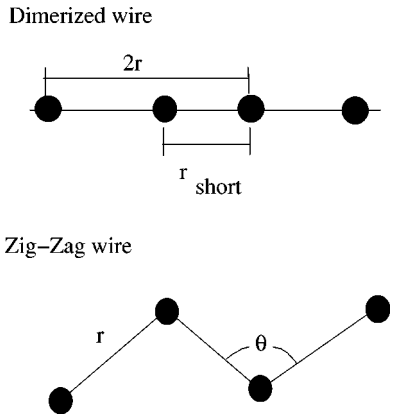


FIG. 3. Geometries of the unsupported dimerized and zigzag wires.

### B. Unsupported dimerized and zigzag Al wires

The next step in our study is to allow the atoms of an unsupported linear Al chain to dimerize and also to form zigzag wires. These geometries are studied because a linear chain of atoms is susceptible to Peierls-like distortions, opening up a small band gap and lowering thereby the total energy. The notations of the geometries studied are presented in Fig. 3. In the dimerized geometry the distance $2r$ between every second atom remains constant, but the atom in the middle of a cell moves in the direction of $r_{short}$ along the wire. In zigzag wires the nearest-neighbor distance $r$ is kept constant while the zigzag angle $\theta$ is varied. When studying the distortions of the spin-polarized chain the distance $r$ is 2.8 Å whereas for the spin-compensated chain the linear equilibrium value of 2.41 Å is used.

According to Table I, the energy of the Al wire increases with dimerization, i.e., the bond-length alternation for the Al chain vanishes or is at least below our error estimate of around 2% of the interatomic distance. We have actually confirmed this energy increase also with the FLAPW calculations. The energy increases more rapidly close to the equilibrium distance corresponding to the nonmagnetic wire than close to the larger distance corresponding to the magnetic wire. It is logical to expect that changes in the geometry of a wire already stretched have a smaller effect on the energy than the changes close to the equilibrium. One can also note

TABLE I. Energies and magnetic moments of dimerized Al wires. The minimum energy for the linear chain of Al atoms defines the energy zero. The spin-compensated and spin-polarized wires are distorted relative to the linear chain of Al atoms with the bond lengths of 2.39 Å and 2.8 Å, respectively.

| Spin compensated | | Spin polarized | | |
|---|---|---|---|---|
| $r_{short}$ (Å) | $E(eV)$ | $r_{short}$ (Å) | $E$ (eV) | $\mu$ ($\mu_B$) |
| 2.41 | 0 | 2.80 | 0.192 | 0.76 |
| 2.35 | 0.007 | 2.75 | 0.189 | 0.76 |
| 2.30 | 0.036 | 2.7 | 0.195 | 0.77 |
| 2.25 | 0.085 | 2.65 | 0.206 | 0.78 |
| 2.2 | 0.160 | 2.6 | 0.221 | 0.80 |

TABLE II. Energies and magnetic moment of zigzag Al wires. The minimum energy for the linear chain of Al atoms defines the energy zero. The spin-compensated and spin-polarized wires are distorted relative to the linear chain of Al atoms with the bond lengths of 2.39 Å and 2.80 Å, respectively.

| Spin compensated | | Spin polarized | | |
|---|---|---|---|---|
| $\theta$ | $E$ (eV) | $\theta$ | $E$ (eV) | $\mu$ ($\mu_B$) |
| 180 | 0 | 180 | 0.192 | 0.76 |
| 170 | −0.008 | 170 | 0.178 | 0.69 |
| 160 | −0.023 | 160 | 0.151 | 0.54 |
| 150 | −0.032 | 150 | 0.101 | 0.25 |
| 140 | −0.019 | 140 | 0.058 | 0.28 |
| 130 | +0.021 | 130 | 0.046 | 0.25 |
| | | 120 | 0.067 | 0.31 |
| | | 110 | 0.076 | 0.24 |

in the case of spin-polarized wires that the magnetic moment grows slightly along dimerization.

Next we consider zigzag wires depicted in Fig. 3. Table II gives the total energies and magnetic moments obtained. The zigzag formation is energetically favorable at the distance $r = 2.41$ Å corresponding to spin-compensated solutions as well as at $r = 2.80$ Å giving magnetic solutions. The values of the equilibrium zigzag angles $\theta$ are around 150° and 130° for the spin-compensated and the magnetic systems, respectively. The deformation is limited by the second-nearest-neighbor atom interactions in the atomic chain. In the magnetic chain, the longer bond length $r$ allows for an angle deformation larger than in the spin-compensated chain.

According to Table II the energies of the chains decrease when the zigzag angle decreases from 180°. Especially for the magnetized chain the decrease is strong and it is accompanied by a decrease in the magnetic moment. The minimum values are obtained at the angle of 120°. To understand this behavior an analysis of the band structure is required. We do this analysis here, in the context of the unsupported Al chains, because this analysis will be the basis to understand the magnetism of the more complicated systems of Al wires on the NaCl(100) surface. The band structure of the magnetic zigzag wire at the equilibrium zigzag angle of 130° is plotted in Fig. 4(a). It is dramatically different from that for the linear chain in Fig. 2. As the zigzag angle $\theta$ decreases, the width of the $s$ band decreases and the band gap at around $-5$ eV increases. The states of the $3p$ bands that cause the magnetization undergo also significant changes. There is no longer a doubly degenerate $p_x - p_y$ band. Two $sp^2$-like bands are formed, the lower of which is occupied both by spin-up and spin-down electrons, whereas the upper $sp^2$-like band is well above the Fermi level. A totally polarized $p_z$ band causes the magnetization. As one-third of the Al $3p$ electrons occupy the $p_z$ band, a magnetic moment of roughly $0.3\mu_B$ can be expected from this interpretation. This value is indeed in agreement with the actual computed result in Table II. At the zigzag angle of 120° [see Fig. 4(b)] the lower $sp^2$-like band becomes polarized at low **k** values. This explains the increase of the magnetic moment at small zigzag angles.

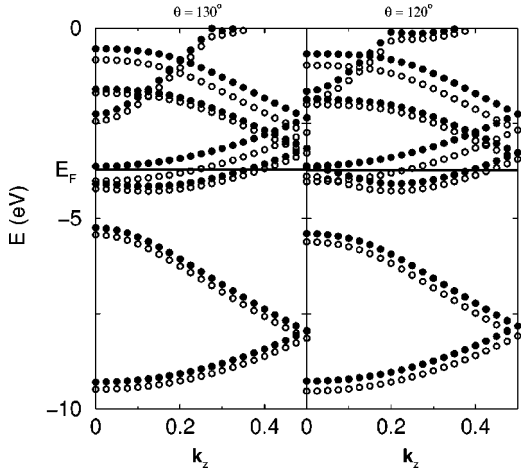


FIG. 4. Band structure of an unsupported magnetic Al nanowire with the zigzag angle of (a) $\theta=130°$ and (b) $\theta=120°$. The nearest-neighbor distance is 2.8 Å. Spin-up and spin-down bands are denoted by open and filled circles, respectively. The Fermi level is given by the horizontal thin line.

### C. Al wire on the NaCl(100) surface

In this section we present our results for an Al wire in equilibrium on the NaCl(100) surface and at the end of of the section we analyze these results using simple model calculations. The NaCl(100) slabs used in the calculations correspond to the atomic layers cut from the perfect bulk crystals with the theoretical lattice constant of 5.68 Å. The omission of the relaxations of Na and Cl ions is justified because we are interested mainly in the effect the surface has on the wire and not vice versa. Before dealing with Al wires on the surface we have made calculations for single isolated Al atoms adsorbed at different sites on NaCl(100). The sites on the top of Na and Cl ions, in the middle of the bridge between the two ions, as well as in the hollow site in the center of four ions have been considered. These calculations show that the properties of the adsorbed Al atoms (adsorption energy and the distance from the surface) do not change remarkably when three NaCl(100) layers are used instead of two or the surface supercell is increased from $3\times3$ to $4\times4$. The following results correspond to two NaCl(100) layers and the $4\times4$ cell, or in the case of the Al wire, the interwire distance is three NaCl lattice constants.

The results for the isolated Al atom on NaCl(100) serve also as guidelines for later calculations dealing with the Al chains on the NaCl(100) surface. The optimized adsorption heights from the surface-layer atoms and the corresponding total energies are given in Table III. The isolated Al atom prefers to be on the top of a Na atom. The total energies are therefore given relative to this system. Thereafter the next favorable site is the hollow one followed by the bridge site. The adsorption of Al on the top of the Cl atom is clearly the most unfavorable case.

The results for the isolated Al on NaCl(100) in mind, we start the simulations for the Al wire commensurate on the NaCl(100) surface. In these calculations there are two rigid layers of Na and Cl ions and the supercell contains two Al atoms. The equilibrium positions of Al atoms obtained reflect

TABLE III. Adsorption of a single Al atom on the NaCl(100) surface. The height $d$ of the adsorbed Al atom from the surface atom layer and the total energies $E$ relative to that for an Al atom on the top of a Na atom are given.

| Position | $d$(Å) | $E$ (eV) |
|---|---|---|
| Top Na | 2.73 | 0.00 |
| Middle face | 2.43 | 0.06 |
| Middle bond | 2.83 | 0.16 |
| Top Cl | 3.83 | 0.32 |

the Al-atom–surface interaction as well as the Al-Al interactions within the wire. It turns out that wires in which the Al atoms sit on the top of nearest Na atoms along the [110] direction as straight or zigzag chains have not the lowest energies. When we optimize the structure of the Al wire by starting from an initial configuration, in which the Al atoms sit slightly randomly close to the adjacent hollow sites, and allow the two Al atoms to move freely both in the horizontal and vertical directions, a strong structural relaxation takes place. The resulting configuration shown in Fig. 5(a) is a zigzag wire in which the Al atoms reside in the bridges between the Na and Cl atoms. The Al atoms are closer to the Cl atoms than the Na atoms so that the zigzag angle $\theta=143°$ and the interatomic distance in the chain is $r=2.99$ Å. The distance to the surface is $d=2.90$ Å. It is exciting that the Al wire in this equilibrium configuration has a magnetic moment of $0.24\mu_b$ per atom. This is just of the order of magnitude expected from Table II for unsupported zigzag wires. Thus the interaction with the NaCl surface does not destroy the magnetic moment of the quasi-one-dimensional Al wire. It would be interesting to confirm this result by FLAPW calculations. Due to the computer resources required, this is presently not possible for us. We have to rely on our test for freestanding wires, showing that the magnetic properties depend only weakly on the the calculation scheme used.

The above results underline the importance of relaxing the positions of the wire atoms on the surface. This kind of relaxation should be performed also when studying the early low-coverage stages of the growth of metal layers on insulating surfaces.[28] The approximation that lateral interactions between adjacent adsorbate atoms are unimportant is maybe not a valid one for all growth patterns.

In order to understand the properties of the above equilibrium wire we have made further calculations using simplified

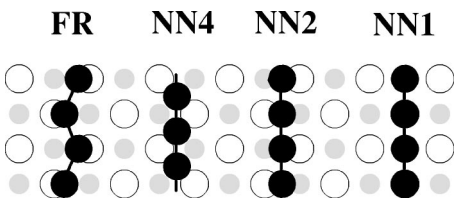


FIG. 5. Geometries of commensurate Al wires on the NaCl(100) surface. The top view of a fully relaxed wire (FR) as well as those of model wires with one (NN1), two (NN2), and four (NN4) nearest-neighbor surface atoms are given. The small gray and large white circles denote the Na and Cl atoms, respectively.

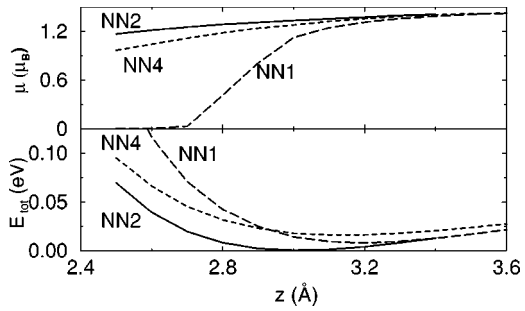


FIG. 6. Commensurate Al wires on NaCl(100). The total energy (lower panel) and the magnetic moment (upper panel) per Al atom are shown as functions of the wire distance from the surface. The long-dashed, solid, and short-dashed curves correspond to the geometries NN1, NN2, and NN4, respectively (see Fig. 5). The minimum energy of NN2 determines the energy zero.

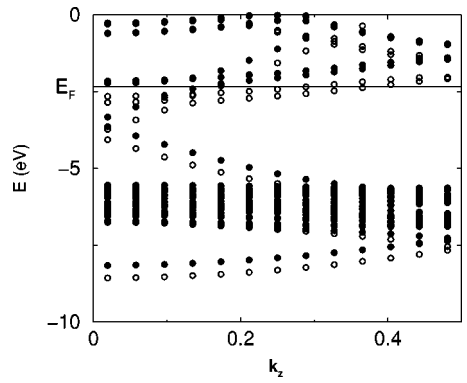


FIG. 7. Band structure of the model Al wire NN2 on NaCl(100) (see Fig. 5) along the wire direction. Spin-up and spin-down bands are denoted by open and filled circles, respectively. The chlorine *s* bands included in our calculations are below −10 eV.

models for linear Al wires on the NaCl(100) surface. In these calculations only one rigid layer of NaCl has been used but the distance between the adjacent wires due to the supercell structure is the same as before. The Al atoms are allowed to relax only perpendicular to the surface. The geometries considered are presented and labeled in Fig. 5. An Al atom has in these geometries one (NN1), two (NN2), or four (NN4) surface ions as nearest neighbors corresponding to atop, bridge, and hollow site wires. The supercells in these simulations contain 12 nonequivalent surface ions and two wire atoms.

The energies of the model wires calculated per one Al atom are shown in the lower panel of Fig. 6 as a function of the distance from the surface layer. The NN2 wire has the lowest equilibrium energy and this is used to define the energy zero. The equilibrium distance is nearly the same as for the fully relaxed zigzag wire discussed above. The NN4 wire has a clearly higher energy. This explains the behavior of our above-discussed simulation starting from Al atoms near the hollow sites. The second lowest-energy minimum is obtained in the NN1 geometry, in which the adjacent Al atoms sit on the top of both Na and Cl surface atoms. Clearly, this geometry in which both Al atoms of the supercell have the same distance from different types of surface atoms is physically not meaningful. Anyway, the fact that the minimum total energy of the NN1 wire is lower than that of the NN4 wire further supports the unstable character of the NN4 wire. In conclusion, the comparison of the results of these model wires with those for single isolated Al atoms on the NaCl(100) surface reflects the balance between the Al-surface interactions and the intrawire interactions.

The upper panel of Fig. 6 shows that all the model wires are magnetic over a wide region around the equilibrium distance. It is interesting to note that the magnetism of the NN1 wire vanishes when the distance to the surface decreases. In order to understand the magnetic properties of these wires as well as those of the fully relaxed wire on NaCl(100) we need to analyze their band structures. The equilibrium band structure of the NN2 wire along the wire direction is shown in Fig. 7. Comparing with Fig. 2 it can be seen that the $3p$ bands around $E_f$ causing the magnetization have lost their degeneracy. However, in contrast to the unsupported zigzag wires in Fig. 4, both of the spin-down $3p$ bands are above the Fermi level. Therefore the magnetic moments of the wires attain values similar to those for unsupported linear wires. The energy bands for NN1 and NN4 geometries show similar features. In the NN2 geometry the occupied spin-up $3p$ bands reach the Fermi level further away from $k_z=0$ than in the NN1 and NN4 geometries. This explains why the magnetic moment is largest in NN2 geometry. When the surface-wire distance is reduced, the unoccupied spin-down bands touch in the NN1 geometry the Fermi level and eventually their low-$k_z$ parts sink below the Fermi level. This is the reason for the gradual decrease of the magnetic moment of the NN1 wire towards shorter distances from the surface.

The band structure of the NN2 wire in Fig. 7 also shows that the Na and Cl bands do not disturb the band structure of the Al wire near the Fermi level. The Na $3s$ bands are well above the Fermi level. The Cl $3p$ bands form, at about 6 eV below the Fermi level, a 1.5-eV-wide region which repells the Al $3s$ bands. This repulsion does not affect the Al $3p$ bands causing the magnetization. Addition of more NaCl layers into the supercell causes larger distortions in the Al $3s$ band, but the above discussion about the origin of the magnetization will not be affected.

In case of the NN2 wire we have tested if dimerization could take place spontaneously. In the test, the distance of the wire from the surface layer is kept constant corresponding to the previously determined equilibrium distance. According to Fig. 6 this is a fair approximation because the energy minima even for the very different geometries occur approximately at the same distance. Then the two Al atoms in a supercell are simultaneously displaced symmetrically in opposite directions to form a dimerized wire. Similarly as in the case of the unsupported linear wires, dimerization increases the energy of the wire. In contrast, a zigzag deformation lowers the energy of the NN2 wire as in the unsupported situation. These notions confirm the results obtained for the fully relaxed Al wire on NaCl(100).

## IV. CONCLUSIONS

We have performed density-functional computations to study electronic and magnetic properties of Al nanowires.

Unsupported atomic chains of Al become magnetic along elongation, in agreement with jellium results. When relaxing, straight wires deform to zigzag wires spontaneously. The zigzag wires exhibit also spontaneous magnetization, although the magnetic moments are lower than those of straight wires.

The results for the unsupported wires form the basis for understanding the properties of nanowires on solid surfaces. Many important features of the electronic structure are conserved when the wire is placed on the solid surface. Metallic nanowires are soft and the role of the surface is then to provide a means to deform in a controlled way the geometry (e.g., the bond length) of the nanowire. As a concrete example we have considered commensurate Al wires on the NaCl(100) surface. A relaxation of the Al ion positions results in a zigzag geometry and the wire conserves its magnetic moment. The resulting properties can be understood by studying the band structures of model wires on a NaCl layer.

An important question is whether the fully relaxed configuration found is stable against relaxation of Al atoms leading to an incommensurate configuration with respect to the NaCl(100) surface. The result depends on the strength of the interwire interaction in comparison with the Al-surface interaction. The lack of spontaneous dimerization for the NN2 model wire supports the stability of the commensurate configuration. Moreover, the full relaxation calculation discussed above, which means starting from slightly random positions for the two Al atoms in a supercell and allowing them to move freely both parallel and perpendicular to the surface, leads to the highly symmetric configuration fully relaxed wire, although the dimerization could also happen. A more complete check of the relative stability of the commensurate and incommensurate wires would require large supercells, which are beyond our present computer resources.

To our knowledge, our calculations for Al wires on NaCl(100) are among the first studies for understanding properties of nanowires on solid surfaces. They show the importance of relaxing the ionic geometry of the wire. In order to gain deeper knowledge more geometries should be tried. For example, an Al wire at the step edge on the NaCl(100) surface would be interesting from the experimental point of view as a way to construct a straight wire. Interesting future topics could also be Al wires on surfaces of different materials, e.g., on silicon.

Studies of nanowires on crystal surfaces are of current scientific interest because such structures can be implemented in future nanotechnological devices. On the other hand, one-dimensional atomic chains on surfaces have been seen during the early stages of the growth of adsorbate layers and they have been shown to exhibit many interesting physical phenomena. We hope that our calculations have enlightened the richness of physical phenomena on these fields and will eventually encourage experiments searching for magnetism of simple metal nanowires on solid surfaces.

## ACKNOWLEDGMENTS

A.A. was financially supported by the EU TMR program (Contract No. ERB4001GT954586). This research has been supported by the Academy of Finland through its Centre of Excellence Programme (2000–2005). We acknowledge the generous computing resources of the Center for the Scientific Computing (CSC), Espoo, Finland. The authors wish to thank G. Kresse for providing the VASP computer programs which made this work possible.

[1] S. Watanabe, Y.A. Ono, T. Hashizume, and Y. Wada, Phys. Rev. B **54**, 17 308 (1996).

[2] P. Segovia, D. Purdle, M. Hengsberger, and Y. Baer, Nature (London) **402**, 504 (1999).

[3] H.W. Yeom, S. Takeda, E. Rotenberg, I. Matsuda, K. Horikoshi, J. Schaefer, C.M. Lee, S.D. Kevan, T. Ohta, T. Nagao, and S. Hasegawa, Phys. Rev. Lett. **82**, 4898 (1999).

[4] G.P. Lopinski, D.D. Wayner, and R.A. Wolkow, Nature (London) **406**, 48 (2000).

[5] R. Losio, K.N. Altmann, and F.J. Himpsel, Phys. Rev. Lett. **85**, 808 (2000).

[6] C. Pampuch, O. Rader, T. Kachel, and W. Gudat, Phys. Rev. Lett. **85**, 2561 (2000).

[7] D.I. Bazhanov, W. Hergert, V. S. Stepanyuk, A. A. Katsnelson, P. Rennert, K. Kokko, and C. Demangeat, Phys. Rev. B **62**, 6415 (2000).

[8] D.M. Eigler and E.K. Schweizer, Nature (London) **344**, 524 (1990).

[9] T.C. Shen, C. Wang, and J.R. Tucker, Phys. Rev. Lett. **78**, 1271 (1997).

[10] P. Gambardella, M. Blanc, H. Brune, K. Kuhnke, and K. Kern, Phys. Rev. B **61**, 2254 (2000).

[11] A. Dallmeyer, C. Carbone, W. Eberhardt, C. Pampuch, O. Rader, W. Gudat, P. Gambardella, and K. Kern, Phys. Rev. B **61**, R5133 (2000).

[12] S.J. Koh and G. Ehrlich, Phys. Rev. B **62**, R10 645 (2000).

[13] L. Pleth Nielsen, F. Besenbacher, I. Stensgaard, and E. Lægsgaard, Phys. Rev. Lett. **74**, 1159 (1995).

[14] S. Watanabe, M. Ichimura, T. Onogi, Y.A. Ono, T. Hashizume, and Y. Wada, Jpn. J. Appl. Phys., Part 2 **36**, L929 (1997).

[15] S. Okada and A. Oshiyama, Phys. Rev. B **62**, R13 286 (2000).

[16] N. Zabala, M.J. Puska, and R.M. Nieminen, Phys. Rev. Lett. **80**, 3336 (1998).

[17] A. Ayuela, J.-L. Mozos, R. M. Nieminen, and M. J. Puska, $\Psi_k$ Newsletter (1998).

[18] A.L. Glebov, J.P. Toennies, and F. Traeger, Phys. Rev. Lett. **82**, 4492 (1999).

[19] G. Kresse and J. Furthmüller, Phys. Rev. B **54**, 11 169 (1996); G. Kresse and J. Furthmüller, *VASP the Guide* (Vienna University of Technology, Vienna, 1999) [http://tph.tuwien.ac.at/~vasp/guide/vasp.html]

[20] P. Blaha, K. Schwarz, and J. Luitz, WIEN97, computer code (Vienna University of Technology, Vienna, 1997) [improved and updated Unix version of the copyrighted WIEN code, which was published by P. Blaha, K. Schwarz, P. Sorantin, and S. B. Trickey, Comput. Phys. Commun. **59**, 399 (1990)].

[21] J.P. Perdew, J.A. Chevary, S.H. Vosko, K.A. Jackson, M.R. Pederson, D.J. Singh, and C. Fiolhais, Phys. Rev. B **46**, 6671 (1992).
[22] D. Vanderbilt, Phys. Rev. B **41**, 7892 (1990); G. Kresse and J. Hafner, J. Phys.: Condens. Matter **6**, 8245 (1994).
[23] G. Makov and M.C. Payne, Phys. Rev. B **51**, 4014 (1995); J. Neugebauer and M. Scheffler, *ibid.* **46**, 16 067 (1992).
[24] H.J. Monkhorst and J.D. Pack, Phys. Rev. B **13**, 5188 (1976).
[25] H. Mehrez and S. Ciraci, Phys. Rev. B **56**, 12 632 (1997).
[26] N. Zabala, M.J. Puska, and R.M. Nieminen, Phys. Rev. B **59**, 12 652 (1999).
[27] G. Rubio, N. Agraït, and S. Vieira, Phys. Rev. Lett. **76**, 2302 (1996).
[28] D. Fuks, S. Dorfman, E.A. Kotomin, Y.F. Zhukovskii, and A.M. Stoneham, Phys. Rev. Lett. **85**, 4333 (2000).